ISSN 2277-2685
IJESR/October-December. 2026/ Vol-16/Issue-4/25-30
Palakurthi Vasundhara / International Journal of Engineering & Science Research
Full Length Article

Advanced Model Predictive Control for Battery Energy Management and SoC Estimation in Electric Vehicles

Palakurthi Vasundhara[1], Chilakala Nagarjun[2], Dr. L. Kishore[3]
[1]Electrical and Electronics Engineering, Sri Chaitanya Institute of Technology and Research, Khammam, India
[2]Electrical and Electronics Engineering, Sri Chaitanya Institute of Technology and Research, Khammam, India
[3]Electrical and Electronics Engineering, Sri Chaitanya Institute of Technology and Research, Khammam, India
Mail Id: vasundharap29@gmail.com[1], chilakalanagarjuna@gmail.com[2], kishorephd724@gmail.com[3]
Accepted 15-11-2026
Author(s) Retains the Copyrights of This Article

Abstract
Battery energy management in electric vehicles (EVs) depends on two coupled tasks: deciding how power is shared between storage devices and knowing how much charge remains. This paper presents a framework that combines a constrained model predictive controller (MPC) with an extended Kalman filter (EKF) for state of charge (SoC) estimation. The vehicle is represented by a lithium-ion pack with a second-order equivalent circuit, supported by a super capacitor bank that absorbs fast power transients. The MPC solves a quadratic problem over a 20 s horizon at 1 s sampling to schedule battery power under power and energy-state limits, while the EKF reconstructs SoC from noisy current and voltage measurements. Both are evaluated on a synthetic 966 s urban, suburban and highway cycle in a numerical block-diagram model implemented in Python. Compared with a battery-only configuration, the MPC lowers peak discharge current from 140.4 A to 54.5 A, RMS current from 35.8 A to 27.6 A and resistive loss from 143.6 kJ to 95.8 kJ. Against a tuned low-pass rule-based split, the reductions are 28.2 %, 6.8 % and 10.3 %. A sensitivity study shows that horizon length and demand preview strongly influence peak-current reduction. The EKF recovers from a 15-point initial SoC error within 3 s and holds an RMSE of 0.14 percentage points despite current bias, sensor noise and parameter mismatch, whereas Coulomb counting retains the initial error. The results are simulation-based and rely on assumed parameters; experimental validation remains to be done.

Keywords: *model predictive control; battery management system; state of charge estimation; extended Kalman filter; hybrid energy storage; electric vehicles*

Introduction

Because the battery supplies all propulsion energy in an electric vehicle (EV), the battery management system (BMS) carries much of the responsibility for safe and efficient operation. Its tasks include state estimation, cell balancing and thermal management [1]. Among these, state of charge (SoC) is the most visible quantity, yet it cannot be measured directly and must be inferred from current and voltage with the help of a battery model [2], [3].

A second challenge concerns how the stored energy is used. Hard acceleration and regenerative braking produce power peaks that raise battery current, resistive loss and ageing stress. Predictive control is attractive here because it handles constraints explicitly. It has been applied to battery charging [4], [5] and to energy management in EV traction systems [6]. Estimation, health monitoring and balancing, however, are typically addressed separately [7].

This work addresses that gap. A battery and supercapacitor hybrid storage system is governed by a constrained model predictive controller (MPC), while an extended Kalman filter (EKF) supplies the SoC estimate from noisy measurements. The objectives are: (i) to formulate a quadratic MPC that reduces battery current stress under power and energy-state limits; (ii) to design an EKF for a second-order equivalent circuit model and quantify its accuracy under noise, bias and parameter mismatch; and (iii) to examine how horizon length and demand preview affect performance and computing effort.

The remainder of the paper is organized as follows. Section 2 reviews related work, Section 3 describes the models, controller and estimator, Section 4 presents and discusses the simulation results, and Section 5 concludes with directions for future work.

Literature Review

Several reviews frame the problem. Ashok et al. examined the control architecture of the BMS, covering battery models and the control approaches used for state estimation, cell balancing and thermal management, and closed with recommendations for open challenges [1]. Laadjal and Cardoso surveyed estimators for EV batteries, listing the Kalman filter and its extended and

unscented variants, particle filters, sliding-mode and H-infinity observers and Luenberger observers, and noting that equivalent-circuit parameters are affected by temperature, C-rate, SoC and ageing [3]. Martí-Florences et al. approached modelling from the state-estimation side, covering the single-particle model and observers, and stressed that SoC and state of health are internal variables that cannot be measured directly [2].

On the estimation side, practical EKF designs are well documented. Rzepka et al. provided a step-by-step EKF for a cell model with two RC elements and hysteresis, and determined the filter settings systematically instead of tuning them empirically [8]. Xie et al. identified the parameters of a second-order RC model in MATLAB/Simulink, built a test platform, and compared EKF-based estimates against the ampere-hour integral method [9].

On the control side, predictive strategies have been applied mainly to charging and traction. Chen et al. cast charging as an MPC problem on a Thevenin model in state-space form, suitable for a low-cost digital signal processor, and reported improvements of 3.25 % in charging time and 0.76 % in average temperature over constant current–constant voltage charging [4]. Li et al. proposed a constraint-triggered PI charging strategy with an ensemble transform Kalman filter that approaches the result of a nonlinear MPC at much lower computational cost [5]. Abdelaal et al. developed a fuzzy-tuned MPC that adjusts the input weight from battery information; against conventional fuzzy and MPC controllers it reduced the SoC drop and state-of-health degradation, and it was tested in real time on a prototype with the NEDC and US06 cycles [6]. Breglio et al. combined SoC and state-of-health estimation with MPC-based active balancing and validated the architecture in simulation under noise, model uncertainty and degradation [7]. At a wider level, Joshal and Gupta noted that the receding-horizon principle lets MPC optimize under constraints in microgrid applications [10].

Three observations follow. First, equivalent-circuit EKFs are mature and robust when carefully tuned. Second, predictive control has been demonstrated for charging, balancing and traction, and the integrated architecture of Breglio et al. shows the value of treating estimation and control together. Third, hybrid storage with an explicit power-split MPC, evaluated with an estimator under sensor imperfections, receives less attention in the works reviewed here. The present study addresses this combination, and it adds a systematic look at prediction horizon and demand preview, which govern both performance and computing effort.

Materials and Methods

Materials

The study is simulation-based; no measured data were used. The EV is a 1,500 kg passenger car (frontal area 2.2 m², drag coefficient 0.29, rolling resistance coefficient 0.010, 0.5 kW auxiliary load). The speed profile is a synthetic composite of urban stop-and-go, suburban and highway segments lasting 966 s (16.7 km, maximum 110.5 km/h) and producing a DC-bus demand between −23.3 kW and 50.1 kW and a net energy of 2.15 kWh. The storage system combines a 96-series, 50 Ah lithium-ion pack represented by a second-order (2-RC) Thevenin model with a 0.4 kWh supercapacitor bank behind a DC/DC converter (efficiency 0.97). All parameters are assumed representative values, not manufacturer data. The model follows the block layout of Fig. 1 and was solved numerically in Python 3 using NumPy, and the quadratic programs were solved with the SLSQP routine of SciPy.

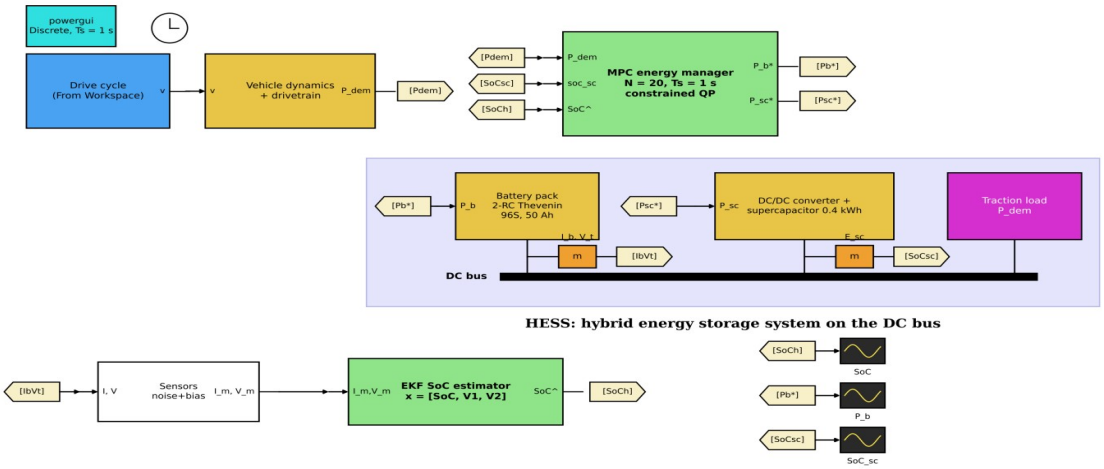

Fig. 1. Simulink-style block diagram of the EV hybrid energy storage model with MPC energy manager and EKF estimator.

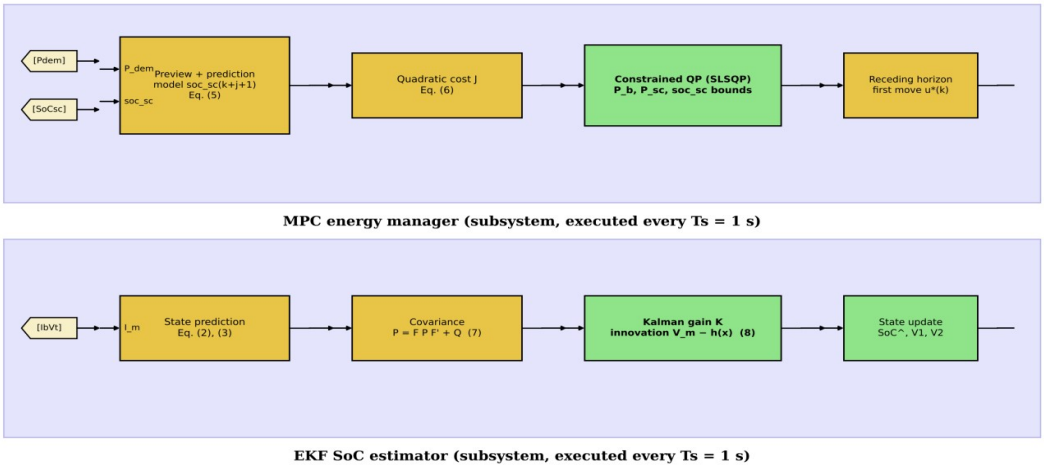

Fig. 2. Internal structure of the MPC energy manager and the EKF estimator.

Procedures

Step 1: vehicle load. The wheel power follows from the speed profile and the longitudinal dynamics, and is converted to DC-bus demand with drivetrain efficiency η_dt = 0.92 in traction and regenerative efficiency η_rg = 0.85 in braking:

P_dem = (m·a·v + 0.5·ρ·C_d·A_f·v^3 + C_rr·m·g·v)/η_dt + P_aux (traction) (1)

where m is the vehicle mass, a the acceleration, v the speed, ρ the air density, C_d the drag coefficient, A_f the frontal area, C_rr the rolling-resistance coefficient and g the gravitational acceleration. In braking, the bracketed term is multiplied by η_rg instead of divided by η_dt.

Step 2: battery model. For discharge current I (positive in discharge), sampling period Δt and capacity Q (Ah), the states evolve as:

SoC(k+1) = SoC(k) − I(k)·Δt/(3600·Q) (2)

V_j(k+1) = e^(−Δt/(R_j·C_j))·V_j(k) + R_j·(1 − e^(−Δt/(R_j·C_j)))·I(k), j = 1, 2 (3)

V_t = N_s·OCV(SoC) − V_1 − V_2 − R_0·I (4)

where V_1 and V_2 are the RC-branch voltages, R_0 the ohmic resistance, N_s the number of series cells and OCV the open-circuit voltage of one cell. For a requested battery power P_b the current is obtained by solving P_b = V_t·I.

Step 3: MPC energy manager. At each sample the controller chooses the battery power sequence P_b(0…N−1). The supercapacitor energy state follows from the power balance, with P_sc = P_dem − P_b and E_sc the bank energy:

soc_sc(k+j+1) = soc_sc(k+j) − (P_dem(k+j) − P_b(k+j))·Δt/E_sc (5)

J = ∑_(j=0)^(N−1) [w_b·P_b(j)^2 + w_d·(P_b(j) − P_b(j−1))^2 + w_s·(soc_sc(j+1) − 0.65)^2] (6)

subject to −35 ≤ P_b ≤ 90 kW, |P_dem − P_b| ≤ 50 kW and 0.25 ≤ soc_sc ≤ 1.00. The first term limits battery current, the second smooths power changes and the third keeps the supercapacitor near a mid-range state so that it can absorb both acceleration and regeneration. The demand over the horizon is taken from a preview of the cycle; a variant that holds the present demand is also tested. Only the first move is applied (receding horizon). Two baselines are used: a battery-only configuration, and a rule-based split in which the battery follows a first-order low-pass filter of the demand (time constant 15 s) with energy guards on the supercapacitor.

Step 4: EKF estimator. With state x = [SoC, V_1, V_2], the filter predicts and updates at every sample:

P(k|k−1) = F·P(k−1|k−1)·F^T + Q (7)

K = P(k|k−1)·H^T·(H·P(k|k−1)·H^T + R)^(−1);
x̂(k) = x̂(k|k−1) + K·(V_m − h(x̂(k|k−1))) (8)

where F and H are the Jacobians of the state transition and of the output function h (Eq. 4), Q and R are the process and measurement noise covariances, and V_m is the measured terminal voltage. The estimator uses measured current corrupted by 0.5 A noise and a 0.5 A bias, voltage noise of 0.5 V, a 2 mV per cell open-circuit-voltage offset, an ohmic resistance 10 % too high, a capacity 3 % too low and an initial SoC of 75 % against a true value of 90 %. Coulomb counting with the same measured current is the reference.

3.3 Analysis

Energy management is judged by peak and RMS battery current, resistive loss (I^2R_0 plus the RC-branch losses), ampere-hour throughput and net SoC change. Estimation is judged by the root-mean-square error (RMSE) after the first 100 s, the mean absolute error, the maximum error and the time needed to stay within 2 percentage points (pp):

RMSE = sqrt((1/n)·∑_(k=1)^n (SoC_hat(k) − SoC(k))^2) (9)

Sensitivity runs vary the horizon (N = 3, 5, 10, 20, 30) and remove the preview. The estimator is further stressed with initial errors of 5 %, 15 % and 30 %, doubled noise, a 30 % ohmic mismatch, a 5 mV per cell OCV offset and an 8 % capacity

mismatch. The weights and the horizon were selected from these runs on the same cycle, so the figures should be read as a design study and not as an independent validation.

Results and Discussion

Fig. 3 shows the cycle used and Fig. 4 the resulting power split. In the battery-only case, demand peaks pass directly to the battery, with a peak discharge current of 140.4 A and a regenerative current of 61.9 A. The rule-based split smooths the demand, but its fixed filter has no knowledge of what is coming and no direct view of the supercapacitor limits. The MPC uses the preview to start unloading the battery before a peak and keeps the supercapacitor state between 28 % and 65 % (Fig. 4, lower panel).

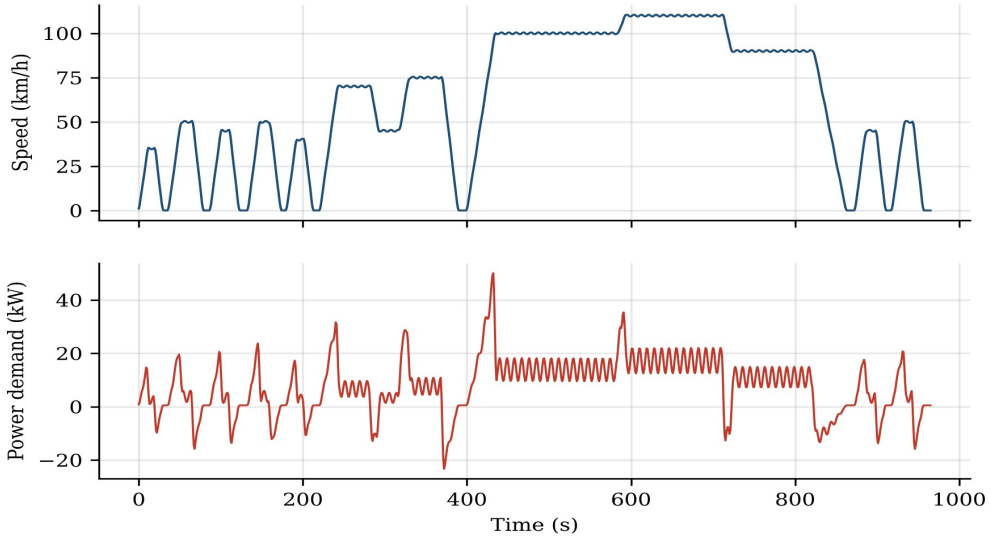

Fig. 3. Synthetic drive cycle and resulting DC-bus power demand.

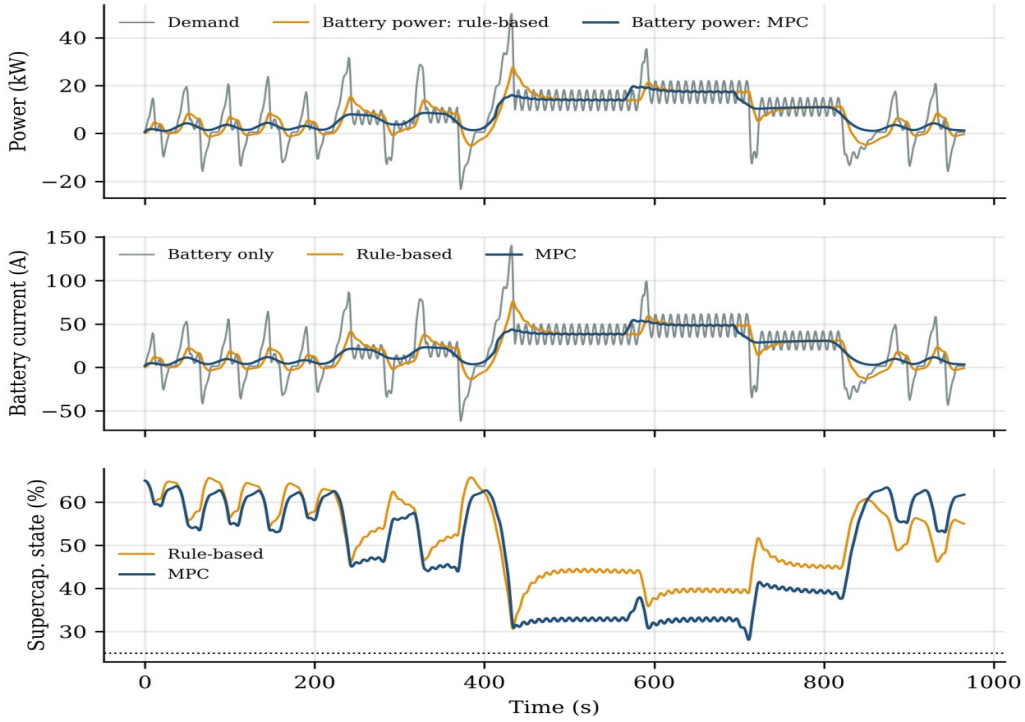

Fig. 4. Power split, battery current and supercapacitor energy state for the three strategies.

Fig. 5 summarize the indicators. Relative to the battery-only configuration, the MPC cuts the peak discharge current by 61.2 %, the RMS current by 22.8 % and the loss by 33.3 %. Relative to the rule-

based split, the reductions are 28.2 %, 6.8 % and 10.3 %, and the battery receives almost no regenerative current because the supercapacitor takes it. The net SoC drop is practically unchanged (11.96 pp against 11.83 pp), which indicates that the benefit comes from redistribution of power over time and not from drawing less energy; the MPC finishes with a slightly higher supercapacitor state, which is consistent with the small difference.

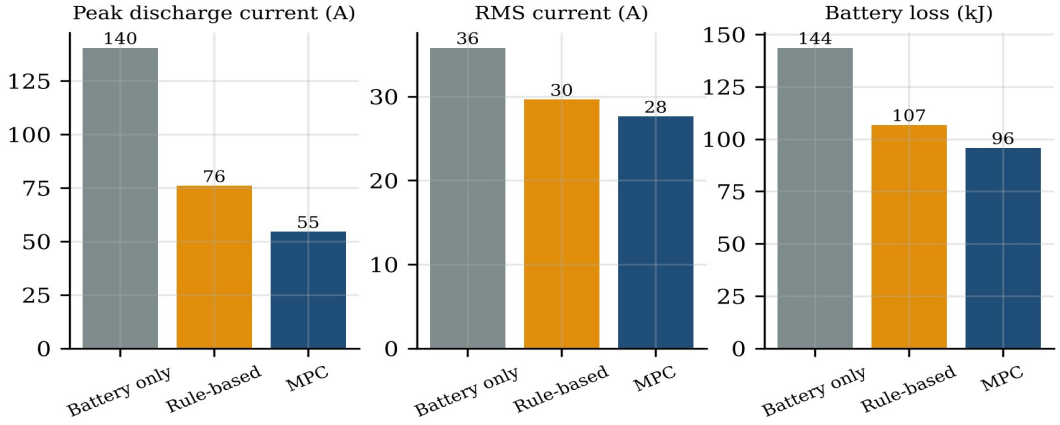

Fig. 5. Battery stress indicators by strategy.

shows that horizon length is the dominant design parameter. Short horizons ($N \leq 5$) behave like the rule-based split because they cannot anticipate the energy needed by the large acceleration events. Peak current falls steeply up to $N = 20$ and then flattens, while computing time keeps rising; $N = 20$ was therefore adopted. Removing the preview doubles the peak current (114.2 A), so the benefit relies on knowledge of upcoming demand, for example from navigation data, and with a constant-demand assumption the advantage over the rule-based split is smaller. In all cases the mean solve time stays at a few milliseconds on a general-purpose processor, well below the 1 s sampling period, although the figure is not representative of embedded hardware.

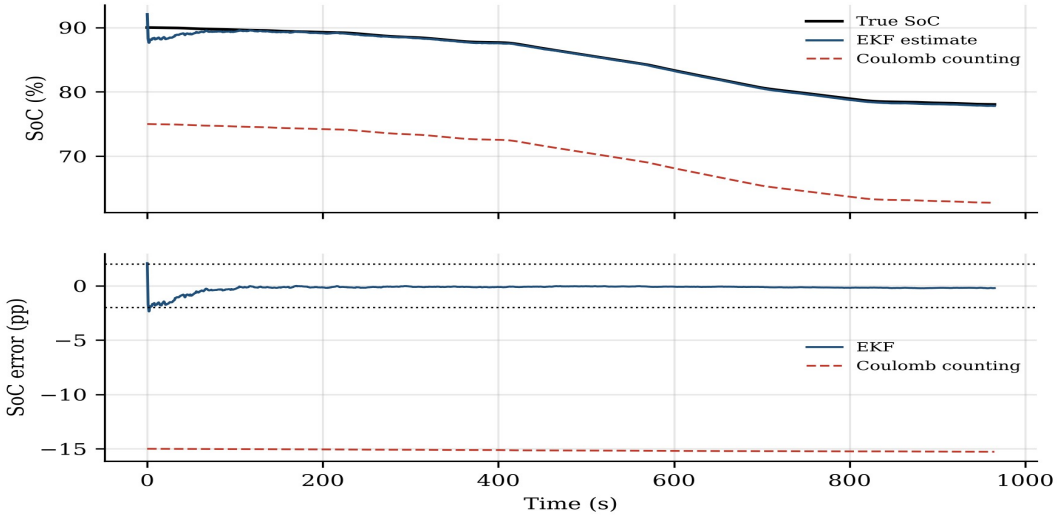

Fig. 6. SoC estimation with 15 % initial error, noise, current bias and parameter mismatch.

Fig. 6 show the estimator results. Starting 15 points away from the true value, the EKF enters the ±2 pp band within 3 s and keeps an RMSE of 0.14 pp and a maximum error of 0.27 pp, whereas Coulomb counting keeps the initial error for the whole drive because it has no measurement correction. Even with a 30 % initial error the EKF settles in 60 s. Parameter mismatch matters more than noise: an OCV offset of 5 mV per cell is the most demanding case (RMSE 0.38 pp, 17 s to converge), because a bias in the voltage map transfers directly to the SoC estimate. These accuracies reflect the steep OCV–SoC slope of the assumed cell and the absence of hysteresis and temperature effects, so they are likely optimistic for real cells, in which Rzepka et al. showed that hysteresis must be modelled explicitly [8].

Comparison with earlier work should be made carefully, because plants, cycles and objectives differ. The direction of the result agrees with Abdelaal et al., who found that making an MPC aware of battery information lowered SoC reduction and degradation relative to conventional controllers [6]; here the information is the supercapacitor energy state and the demand preview. The gains reported by Chen et al. for MPC charging (3.25 % in time, 0.76 % in temperature) address another objective and cannot be compared numerically [4]. The second-order model used by the EKF is consistent with the choices of Xie et al. and Rzepka et al. [9], [8], and the combined evaluation of estimator and controller follows the integrated view of Breglio et al. [7], although with a different plant and task.

Conclusion and Future Work

This paper combined a constrained MPC for battery and supercapacitor power sharing with an EKF for SoC estimation and evaluated both on a synthetic 966 s drive cycle. With a 20 s horizon and demand preview, the MPC reduced peak battery current by 61.2 % against a battery-only system and by 28.2 % against a tuned low-pass rule, with RMS current and resistive loss lower by 6.8 % and 10.3 % in the second comparison. Horizon length and preview were shown to be decisive. The EKF corrected a 15-point initial error within 3 s and kept the RMSE at 0.14 pp under noise, bias and moderate parameter mismatch.

The contribution is a transparent, reproducible formulation that links energy management and state estimation in one study. The limits are equally clear: the parameters are assumed, the cycle is synthetic, temperature and hysteresis are not modelled, and the preview is idealized. Future work should validate the models on measured cell and drive data, add thermal and ageing terms to the MPC cost, use the EKF estimate inside the controller loop, test forecast errors in the demand preview, and implement the solver on embedded hardware.

References

[1] Ashok, B., Kannan, C., Mason, B., Ashok, S. D., et al. (2022). Lithium-ion-battery-powered electric vehicles: A comprehensive review on control strategy architecture of battery management system. *Energies*, *15*(12), 4227. https://doi.org/10.3390/en15124227

[2] Martí-Florences, M., Cecilia, A., & Costa-Castelló, R. (2023). Modelling and estimation in lithium-ion batteries: A literature review. *Energies*, *16*(19), 6846. https://doi.org/10.3390/en16196846

[3] Laadjal, K., & Cardoso, A. J. M. (2021). Estimation of lithium-ion batteries state-condition in electric vehicle applications: Issues and state of the art. *Electronics*, *10*(13), 1588. https://doi.org/10.3390/electronics10131588

[4] Chen, G.-J., Liu, Y.-H., Cheng, Y.-S., & Pai, H.-Y. (2021). A novel optimal charging algorithm for lithium-ion batteries based on model predictive control. *Energies*, *14*(8), 2238. https://doi.org/10.3390/en14082238

[5] Li, Y., Vilathgamuwa, D. M., Wikner, E., Wei, Z., Zhang, X., Thiringer, T., Wik, T., & Zou, C. (2021). Electrochemical model-based fast charging: Physical constraint-triggered PI control. *IEEE Transactions on Energy Conversion*, *36*(4), 3208–3220. https://doi.org/10.1109/TEC.2021.3065983

[6] Abdelaal, A. S., Mukhopadhyay, S., & Rehman, H. (2022). Battery energy management techniques for an electric vehicle traction system. *IEEE Access*, *10*, 84015–84037. https://doi.org/10.1109/ACCESS.2022.3195940

[7] Breglio, L., Fiordellisi, A., Gasperini, G., Iodice, G., Palermo, D., Tufo, M., Ursumando, F., & Mele, A. (2024). A model-based strategy for active balancing and SoC and SoH estimations of an automotive battery management system. *Modelling*, *5*(3), 911–935. https://doi.org/10.3390/modelling5030048

[8] Rzepka, B., Bischof, S., & Blank, T. (2021). Implementing an extended Kalman filter for SoC estimation of a Li-ion battery with hysteresis: A step-by-step guide. *Energies*, *14*(13), 3733. https://doi.org/10.3390/en14133733

[9] Xie, J., Wei, X., Bo, X., Zhang, P., Chen, P., Hao, W., & Yuan, M. (2023). State of charge estimation of lithium-ion battery based on extended Kalman filter algorithm. *Frontiers in Energy Research*, *11*, 1180881. https://doi.org/10.3389/fenrg.2023.1180881

[10] Joshal, K. S., & Gupta, N. (2023). Microgrids with model predictive control: A critical review. *Energies*, *16*(13), 4851. https://doi.org/10.3390/en16134851